The Journal of Neuroscience, March 15, 1996, 16(6):2044–2056

Immunocytochemical Localization of Group III Metabotropic Glutamate Receptors in the Hippocampus with Subtype-Specific Antibodies

Stefania Risso Bradley,[1] Allan I. Levey,[2] Steven M. Hersch,[2] and P. Jeffrey Conn[1]

Departments of [1]Pharmacology and [2]Neurology, Emory University School of Medicine, Atlanta, Georgia 30322

The metabotropic glutamate receptors (mGluRs) mGluR4 and mGluR7 have been postulated to serve as presynaptic autoreceptors in the hippocampal formation. The cellular and synaptic localization of these proteins in the hippocampus, however, is not known. Polyclonal antibodies that specifically react with mGluR4a or mGluR7 were produced and used for immunocytochemical localization of these receptor proteins. Immunoblot analysis with mGluRs expressed in stably transfected baby hamster kidney cells suggests that each of the antibodies reacts specifically with the appropriate mGluR subtype but not with other mGluRs. Both antibodies recognized native proteins in rat brain with molecular weights similar to the molecular weights of the bands in mGluR-transfected cell lines. The distribution of mGluR4a immunoreactivity was fairly uniform in all brain regions. Immunoreactivity for mGluR7 was variable in different brain regions and closely paralleled the previously reported distribution of mGluR7 mRNA. Immunocytochemistry with light and electron microscopy (EM) revealed that immunoreactivities for mGluR4a and mGluR7 are widely but differentially distributed throughout the hippocampal formation. Staining with antibodies directed against mGluR4a was intense in cell bodies and dendrites of pyramidal cells, granule cells, and scattered interneurons. Analysis at the EM level revealed postsynaptic mGluR4a localization at asymmetrical (presumably glutamatergic) synapses and presynaptic localization at both asymmetrical and symmetrical synapses. Immunoreactivity for mGluR7 revealed largely presynaptic localization of this receptor at asymmetrical but not symmetrical synapses. These data are consistent with a largely presynaptic role of mGluR7 in the hippocampus and suggest that mGluR4 may have both presynaptic and postsynaptic functions.

Key words: metabotropic glutamate receptor; hippocampus; mGluR7; mGluR4; L-AP4; immunocytochemistry; autoreceptors

The hippocampus is a limbic cortical structure that plays an important role in a number of normal physiological processes, including learning and memory, as well as in various pathological conditions. The hippocampus is viewed commonly as a relatively simple circuit consisting of three major excitatory synapses, each of which employs glutamate as a neurotransmitter (Brown and Zador, 1990). Glutamate elicits fast excitatory synaptic responses at each of these synapses by activating ligand-gated cation channels known as ionotropic glutamate receptors. In recent years, it has become clear that glutamate also activates G-protein-linked receptors, referred to as metabotropic glutamate receptors (mGluRs), suggesting that glutamate can modulate transmission and neuronal excitability at the same synapses at which it elicits fast excitatory synaptic responses (for reviews, see Conn et al., 1995; Pin and Duvoisin, 1995).

A great deal of progress has been made in defining various presynaptic and postsynaptic physiological effects of mGluR agonists in the hippocampus (for reviews, see Conn et al., 1994, 1995). Relatively little is known, however, about the synaptic localization and physiological roles of the different mGluR subtypes. To date, eight mGluR subtypes have been identified by molecular cloning, and these receptors can be placed into three groups on the basis of sequence homology, coupling to second messenger systems, and pharmacological profiles (for reviews, see Suzdak et al., 1994; Pin and Duvoisin, 1995). Group I mGluRs include mGluR1 and mGluR5, which couple primarily to increases in phosphoinositide hydrolysis in expression systems. The group II mGluRs, including mGluR2 and mGluR3, and the group III mGluRs, including two splice variants of mGluR4 (mGluR4a and mGluR4b), mGluR6, mGluR7, and mGluR8, all couple to inhibition of cAMP production in expression systems.

Group III mGluRs have been postulated to serve as presynaptic autoreceptors involved in reducing glutamate release from presynaptic terminals (Glaum and Miller, 1994). For instance, in hippocampus, the selective group III mGluR agonist 2-amino-4-phosphonobutyrate (L-AP4) reduces synaptic transmission at excitatory synapses (Koerner and Cotman, 1981; Ganong and Cotman, 1982; Lanthorn et al., 1984; Baskys and Malenka, 1991; Gereau and Conn, 1995a,b). *In situ* hybridization studies reveal that two of the group III mGluRs, mGluR4 and mGluR7, are expressed in hippocampus, suggesting that one or both of these subtypes may serve as autoreceptors in this structure (Nakajima et al., 1993; Tanabe et al., 1993; Okamoto et al., 1994; Saugstad et al., 1994; Duvoisin et al., 1995). *In situ* hybridization localizes mRNA rather than receptor proteins, however, and gives no insight into the presynaptic versus postsynaptic localization of receptors at identified synapses. In the present studies, we have produced and characterized two sets of affinity-purified polyclonal

Received Dec. 8, 1995; revised Dec. 15, 1995; accepted Dec. 29, 1995.

This work was supported by National Institutes of Health Grants NS-28405 and NS-31373 and a grant from the Council for Tobacco Research. We thank Betty Haldeman of Zymogenetics for generously supplying cell lines expressing mGluR1 and mGluR4. The cell line expressing mGluR7 was generously supplied by Dr. Thomas Segerson, Vollum Institute. We also thank Craig J. Heilman, Dr. Howard D. Rees, Hong Yi, and Sharon M. Edmunds for assistance at different stages of these studies, and Dr. Jit Patel, Zeneca Pharmaceuticals, for supplying crude antisera.

Correspondence should be addressed to Dr. P. Jeffrey Conn, Department of Pharmacology, Rollins Research Building, Emory University School of Medicine, Atlanta, GA 30322.

Copyright © 1996 Society for Neuroscience 0270-6474/96/162044-13$05.00/0

rabbit antibodies, one of which specifically interacts with mGluR4a and the other with mGluR7. Use of these antibodies for immunocytochemical localization of mGluR4a and mGluR7 suggests that these receptors have highly complementary localization in the hippocampal formation and are likely to serve different pre- and postsynaptic roles in regulating hippocampal function.

MATERIALS AND METHODS

Production and characterization of polyclonal antibodies that specifically interact with mGluR4a or mGluR7. Antibodies were generated against synthetic peptides corresponding to the putative intracellular C-terminal domains of mGluR4a and mGluR7. Rabbit polyclonal antisera were prepared and affinity-purified as described by Blackstone et al. (1992). Oligopeptides corresponding to the C-terminal regions of mGluR4a and mGluR7 were synthesized on a peptide synthesizer (model 380A, Applied Biosystems, Foster City, CA) and purified by HPLC. An N-terminal lysine was added to each peptide to facilitate coupling to the carrier protein. The peptides had the amino acid sequences listed in Table 1.

Peptides were coupled to keyhole-limpet hemocyanin (KLH) with glutaraldehyde for immunizations. The peptide conjugates were mixed with Freund's adjuvant and injected into three or four subcutaneous dorsal sites (0.5 mg peptide in 1 ml). Two New Zealand white rabbits (3–9 months old) were immunized with each peptide for polyclonal antibody production (Research Genetics, Huntsville, AL). Blood was obtained 4, 8, and 10 weeks after the immunization and was clotted; the serum was collected by centrifugation and stored at −80°C. Antibodies were affinity-purified on the respective peptides coupled to bovine serum albumin or thyroglobulin and immobilized on Affi-Gel (Bio-Rad, Richmond, CA) resin, as described by Ciliax et al. (1994).

Brain dissections. Male Sprague–Dawley rats (200–250 gm) were killed by decapitation, and their brains were removed and dissected on ice. The brain was hemisected, and the hippocampus was dissected as described by Glowinski and Iversen (1966). The cortex ventral to the rhinal fissure was dissected away from the remaining cortex, and after removal of the entorhinal cortex, this cortical section was divided into two portions referred to as limbic forebrain (LF) and piriform cortex/amygdala (PC/A). The remaining cortical tissue is referred to as neocortex. The LF consisted of the portion rostral to the posterior border of the lateral olfactory tract and contained rostral portions of the PC, olfactory tubercle, and nucleus accumbens. PC/A contained caudal PC and amygdaloid structures. Striatum was dissected as described by Blumberg et al. (1976). Other areas were dissected according to Glowinski and Iversen (1966).

Immunoblot analysis. Baby hamster kidney (BHK) cells stably transfected with mGluR1a and mGluR4a, as described previously (Kristensen et al., 1993; Thomsen et al., 1993), were generously supplied by Betty Haldeman (Zymogenetics, Seattle, WA). BHK cells stably transfected with mGluR7 (Saugstad et al., 1994) were generously supplied by Dr. Thomas Segerson (Vollum Institute, Portland, OR). Membranes prepared from transfected BHK cells and from rat brain regions were used for immunoblot studies with the mGluR-directed antibodies. Adult male Sprague–Dawley rats were killed, and microdissected brain regions were homogenized immediately with a Brinkmann Polytron (Brinkmann Instruments, Westbury, NY) in 10 mM Tris and 1 mM EDTA, pH 7.4, containing 2 μg/ml leupeptin, 2 μg/ml aprotinin, and 2 μg/ml pepstatin A. The homogenates were centrifuged at 2250 × *g* for 5 min, and the supernatants were decanted and centrifuged at 13,000 × *g* for 30 min. The membrane pellets were resuspended, the protein concentration was determined, and the membranes were kept at −70°C until use. Rat brain or BHK cell membranes were subjected to SDS-PAGE (10% acrylamide) and transferred to Immobilon-P membranes (Millipore, Bedford, MA) by electroblotting, as described by Towbin et al., (1979). The blots were blocked with 5% nonfat dry milk in Tris-buffered saline (TBS) (20 mM Tris-HCl in 137 mM NaCl, pH 7.4) at room temperature for 30 min. Blots were then incubated overnight at 4°C with affinity-purified mGluR antibodies (0.5 μg/ml) in TBS. Membranes were then rinsed and incubated for 30 min with peroxidase-conjugated goat anti-rabbit IgG (Bio-Rad) at room temperature. After several washes in TBS, immunoreactive proteins were visualized with enhanced chemoluminescence (Amersham, Buckinghamshire, UK), as recommended by the manufacturer. For preadsorption experiments, antibodies were preabsorbed with 10 μg/ml homologous peptide for 1 hr at room temperature. Deglycosylation experiments were performed using peptide *N*-glycosidase F (PNGase F) (1000 U; New England Biolabs, Beverly, MA), as suggested by the manufacturer.

Immunocytochemistry. Immunohistochemistry was performed using well established methods (Levey et al., 1991; Martin et al., 1992; Hersch et al., 1995). For examination at the light microscopic level, adult male Sprague–Dawley rats (n = 10) were anesthetized with 30% chloral hydrate and transcardially perfused with 3% paraformaldehyde followed by 10% sucrose (200–250 ml of each). Rat brains were removed and cryoprotected in 30% sucrose at 4°C in 0.1 M phosphate buffer, pH 7.6, for 48 hr at 4°C, frozen on dry ice, and sectioned at 40–50 μM on a freezing sliding microtome. Sections were collected in 50 mM TBS, pH 7.2, at 4°C. Tissue sections through the entire hippocampal formation and related structures were processed for immunocytochemistry. Sections were preblocked in TBS with 4% normal goat serum (NGS) and avidin (10 μg/ml) for 30 min and subsequently in TBS with NGS and biotin (50 μg/ml) for another 30 min. The sections were then incubated with primary antibody (0.5–2.0 μg/ml) in TBS and 2% NGS for two or three nights at 4°C. The avidin-biotin-peroxidase method (Vectastain Elite ABC kit, Vector Laboratories, Burlingame, CA) was used to detect mGluR4a and mGluR7 immunoreactivity. The tissue was rinsed several times in TBS, and the peroxidase reaction was developed in 0.05% diaminobenzidine (DAB) and 0.01% H_2O_2 for 10–15 min. Sections were rinsed finally in TBS and mounted on subbed slides. Sections were dehydrated in alcohols, defatted in xylene, and coverslipped for analysis.

Control experiments were performed in which sections were incubated in TBS without primary antibody. Further control experiments were performed in which primary antibody was preincubated (10 μg/ml for 1 hr at room temperature) with either the homologous peptide or the peptide corresponding to the C-terminal sequence of the other of the two receptors under investigation.

For EM, rats (n = 3) were perfused with 200 ml of 3% paraformaldehyde and 0.1% glutaraldehyde in 0.1 M phosphate buffer, pH 7.6. Brains were kept for 1 hr at 4°C and then sectioned at 40 μm using a vibratome (Technical Products International, St. Louis, MO). Sections were collected in 0.1 M phosphate buffer and then rinsed several times with TBS (10 min each rinse) before being processed as described for light microscopy. After the treatment with 0.05% DAB and 0.01% H_2O_2 for 10–15 min, the hippocampi were dissected and rinsed several times in TBS. Sections were then incubated overnight in 2% glutaraldehyde in 0.1 M phosphate buffer. After rinsing the hippocampi twice for 10 min in phosphate buffer and then in cacodylate buffer (0.1 M), they were postfixed in 1% osmium tetroxide in 0.1 M cacodylate buffer for 30 min. Slices were then rinsed twice for 10 min in 0.1 M cacodylate buffer, followed by a rinse in 0.05 M acetate buffer. Slices were block-stained overnight in aqueous 2% uranyl acetate, followed by a rinse in 0.05 M acetate buffer. The tissue was then dehydrated in graded ethanols and finally in propylene oxide for 5 min before overnight incubation in Epon 1:1 propylene oxide. The sections were finally embedded in Epon resin between glass slides and left at 60°C for 2 d. Blocks were dissected from different areas of the hippocampus and mounted on stubs and sectioned using an ultramicrotome (RMC MT5000 or Reichert Ultracut). Ultrathin sections were collected on uncoated copper mesh grids for analysis with EM (JEOL 100C).

Table 1. Amino acid sequences of C-terminal regions of metabotropic glutamate receptors

mGluR1a	NVTYASVILRDYKQSSSTL
mGluR2	FVPTVCNGREVVDSTTSSL
mGluR3	YVPTVCNGREVLDSTTSSL
mGluR4a	KTPALATKQTYVTYTNHAI
mGluR5	SPKYDTLIIRDYTQSSSSL
mGluR6	KKTSTMAAPPQNENAEDAK
mGluR7	DKNSPAAKKKYVSYNNLVI
mGluR8	ETNTSSIKTTYISYSDHSI

Amino acid sequences for peptides corresponding to C-terminal regions of mGluR4a and mGluR7 (underlined) used to immunize rabbits for polyclonal antibody production. The sequences of these peptides are compared with the sequences of the other metabotropic glutamate receptors in the same C-terminal region.

RESULTS

Immunoblot analysis

Affinity-purified antibodies directed against either mGluR4a or mGluR7 were characterized by Western blotting analysis with membranes (100 μg protein) from rat brain, control (untrans-

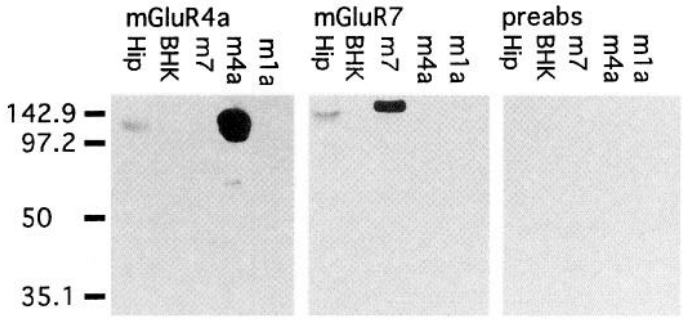

Figure 1. Molecular specificity of mGluR7 and mGluR4a antibodies. Western blot analysis was used with polyclonal antibodies directed against mGluR7 or mGluR4a to determine immunoreactivity in membranes from rat hippocampus (*Hip*), control BHK cells (*BHK*), BHK cells transfected with mGluR7 (*m7*), mGluR4a (*m4a*), or mGluR1a (*m1a*). Blots were incubated with mGluR4a antibodies (*left*), mGluR7 antibodies (*middle*), or antibodies that were preabsorbed with 10 μg/ml homologous peptide (*right*). The *right panel* shows immunoreactivity with mGluR4a-directed antibodies after preadsorption with the peptide corresponding to the sequence of the C-terminal region of mGluR4a. The same result was obtained for mGluR7 (not shown). Molecular weight standards are designated at *left* (in kDa).

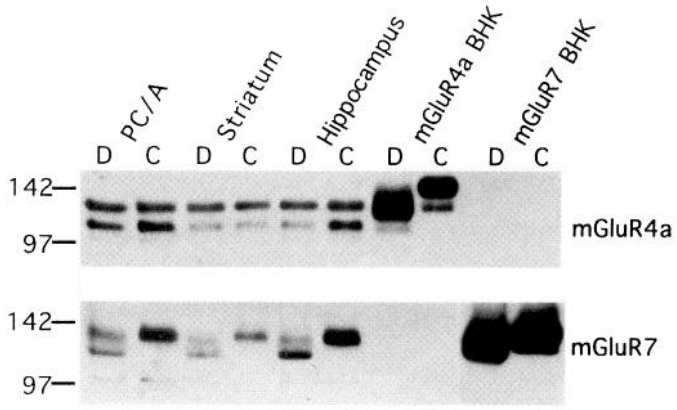

Figure 3. Effect of deglycosylating enzyme treatment on mGluR4a and mGluR7 immunoreactivity. Western blot analysis was performed with antibodies directed against mGluR4a (*top*) or mGluR7 (*bottom*) with membranes from rat piriform cortex/amygdala (*PC/A*), striatum (*Striatum*), hippocampus (*Hippocampus*), and BHK cells transfected with mGluR4a (*mGluR4a BHK*) or mGluR7 (*mGluR7 BHK*). The membranes were treated previously with (*D*) or without (*C*) PNGase F (1000 U) for 4 hr at 37°C. Molecular weight standards are designated at *left* (in kDa).

fected) BHK cells, and BHK cells transfected with either mGluR1a, mGluR4a, or mGluR7. Affinity-purified antibodies directed against mGluR4a reacted with a band at 117 KDa and a second lighter band (at 108 KDa) in homogenates of BHK cells transfected with the mGluR4a. Antibodies directed against mGluR7 reacted with a single band (at 129 KDa) in homogenates of BHK cells transfected with mGluR7 (Fig. 1). The mobilities of these proteins were consistent with the predicted molecular weight of mGluR4a and mGluR7 on the basis of their amino acid sequences. In contrast, neither mGluR4a- nor mGluR7-directed antibodies reacted with nontransfected BHK cells or BHK cells transfected with the other mGluRs tested. Preadsorption of either antibody with homologous peptide totally abolished all immunoreactive bands, as is shown in Figure 1 for mGluR4a.

Both antibodies also recognized native proteins in rat hippocampal homogenates that had molecular weights similar to those of the proteins recognized in transfected cells (Fig. 1). The

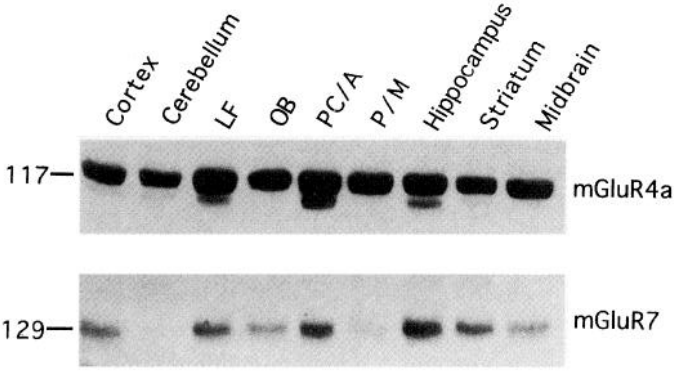

Figure 2. Regional distribution of mGluR4a and mGluR7 immunoreactivity in rat brain. Western blot analysis was used to determine immunoreactivity with antibodies directed against mGluR4a (*top*) and mGluR7 (*bottom*) in membranes (100 μg of protein) from several regions of rat brain. Regions that were analyzed included neocortex (*Cortex*), cerebellum (*Cerebellum*), limbic forebrain (*LF*), olfactory bulb (*OB*), piriform cortex/amygdala (*PC/A*), pons/medulla (*P/M*), hippocampus (*Hippocampus*), striatum (*Striatum*), and midbrain (*Midbrain*). Molecular weight standards are designated at *left* (in kDa).

regional distributions of mGluR4a and mGluR7 were determined in a number of dissected brain regions (Fig. 2). Antibodies directed against mGluR4a reacted with two distinct bands in all limbic regions examined (hippocampus, PC, and LF) but generally reacted with a single band in nonlimbic regions. With longer exposures in some experiments, however, mGluR4a-directed antibodies also reacted with a faint second band in nonlimbic areas. The distribution of mGluR4a was fairly uniform in all brain regions examined. Antibodies directed against mGluR7 reacted with a single band in homogenates from many brain regions. The strongest immunoreactivity was in hippocampus and the regions containing PC/A. Somewhat lower immunoreactivity was seen in cerebral cortex, striatum, midbrain, and olfactory bulb. Faint immunoreactivity was seen in pons/medulla, and cerebellum was devoid of detectable immunoreactivity.

Although mGluR4a- and mGluR7-directed antibodies react with bands in appropriately transfected BHK cells and in rat brain homogenates, there is a slight difference in the molecular weights of the immunoreactive bands in these two preparations (Fig. 1). Thus, the immunoreactive bands in transfected BHK cells have apparent molecular weights that are slightly higher than those in rat brain homogenates. One possible explanation for this finding is that there could be differences in the post-translational modifications of the receptors in BHK cells and rat brain. To determine whether N-linked glycosylation might account for the differences between mGluR-immunoreactivity in BHK cells and rat brain, homogenates were treated with the deglycosylating enzyme PNGase F and analyzed by immunoblotting. Treatment of mGluR4a-transfected BHK cells with PGNase F resulted in a shift in the molecular weights of the two bands to an intense band that corresponds directly with the higher molecular weight band seen in rat brain homogenates and a lighter band that corresponds with the lower molecular weight band seen in rat brain homogenates (Fig. 3, *top*). This suggests that the differences in molecular weights between BHK cells and rat brain homogenates can be explained by differences in glycosylation in the different cell types. PNGase F did not induce a shift in the molecular weights of the immunoreactive bands in rat brain homogenates, however,

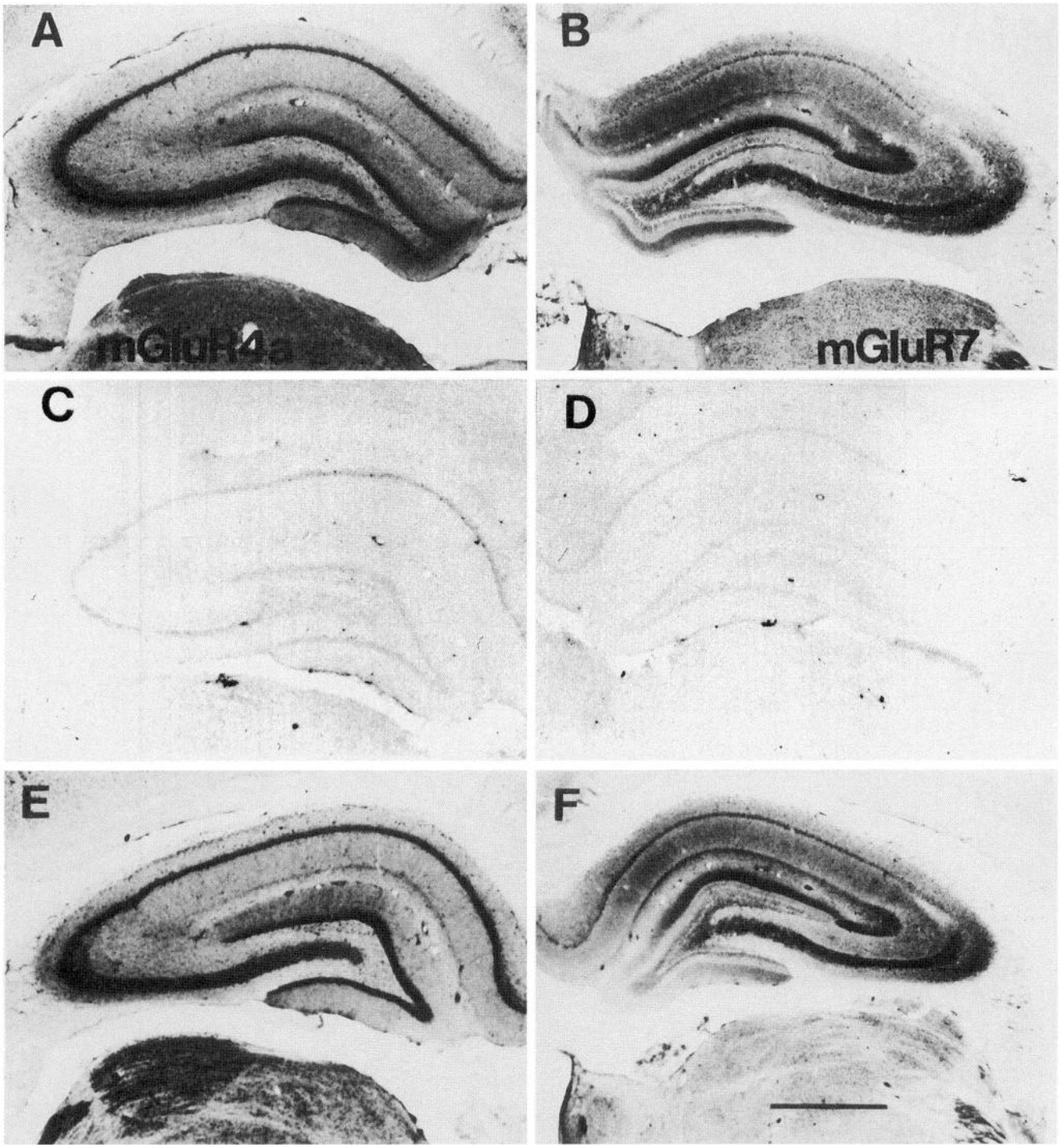

Figure 4. Immunocytochemical analysis of mGluR4a and mGluR7 in rat hippocampus. *A* and *B* show low-magnification immunocytochemical analysis of staining with antibodies directed against mGluR4a (*A*) and mGluR7 (*B*) in sections of rat brain containing the hippocampal formation. *C* and *D* show staining with mGluR4a and mGluR7 antibodies that were preabsorbed with 10 μg/ml homologous peptide. In the section shown in *E*, mGluR4a antibody was preabsorbed with 10 μg/ml mGluR7 peptide. In the section shown in *F*, mGluR7 antibody was preabsorbed with 10 μg/ml mGluR4 peptide. Scale bar (shown in *F*), 1 mm.

suggesting that the differences in molecular weights in these bands do not correspond to differences in PGNase F-sensitive glycosylation states. The finding that both of these bands correspond directly to bands seen in mGluR4a-expressing BHK cells (but not control BHK cells or cells transfected with other mGluRs), however, increases confidence that each of these bands represents a translation product of the mGluR4a gene.

As with mGluR4a, treatment of mGluR7-expressing BHK cells with PGNase F induced a shift in the mGluR7-immunoreactive band to a lower molecular weight (Fig. 3). In contrast to mGluR4a, however, PGNase F treatment also induced a shift of the immunoreactive band seen in rat brain homogenates. The molecular weight of the deglycosylated immunoreactive product in BHK cells corresponds nicely with that of the immunoreactive

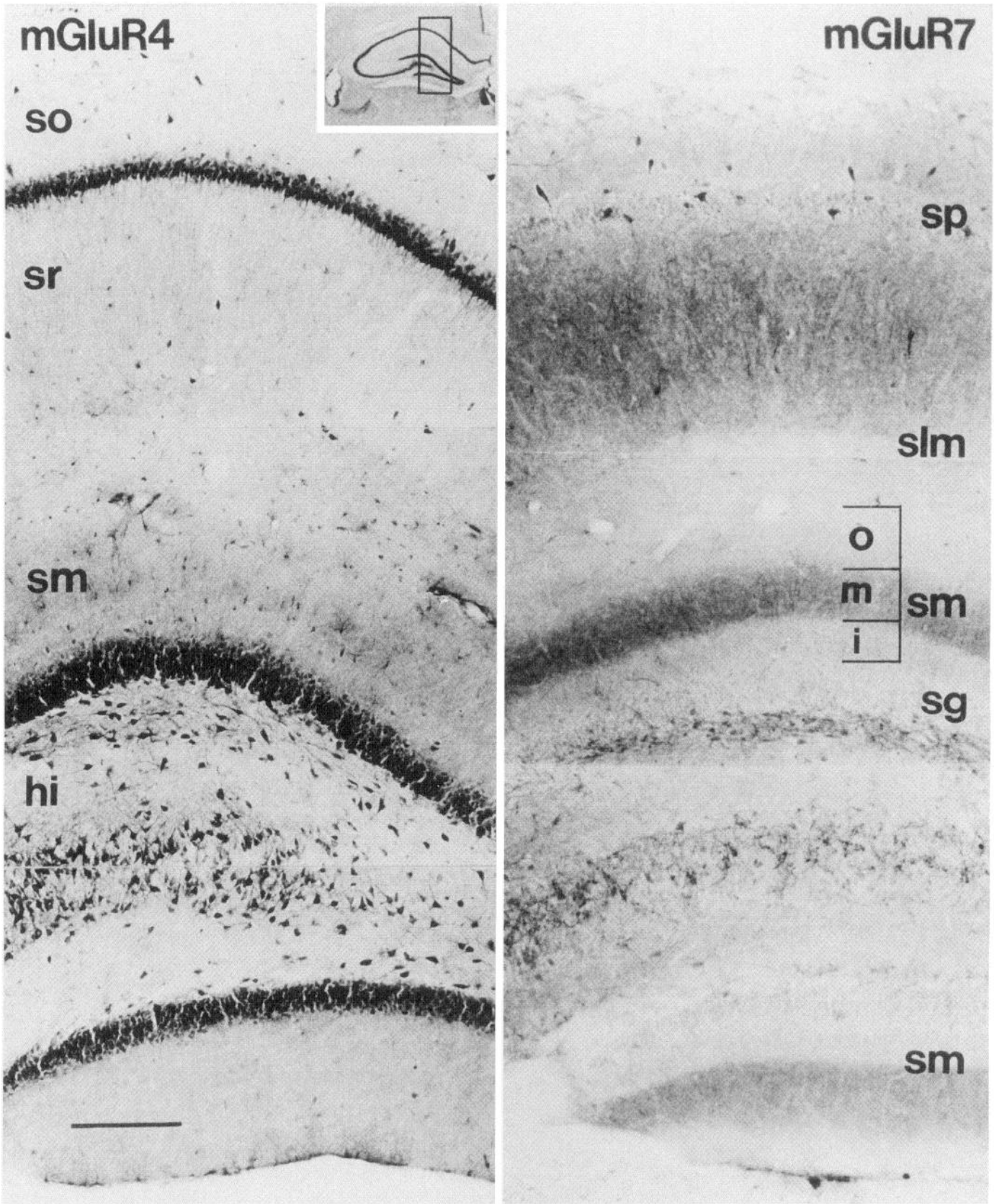

Figure 5. Immunocytochemical staining of a section through the hippocampal formation containing area CA1 and the dentate gyrus. Staining with antibodies directed against mGluR4a (*left*) and mGluR7 (*right*) is shown in an area of the hippocampal formation represented in the *box* shown in the *inset* at the *upper edge* of the figure. From the top, the hippocampus proper is seen with the stratum oriens (*so*), stratum pyramidale (*sp*), stratum radiatum (*sr*), and stratum lacunosum-moleculare (*slm*). Below the *slm* is the dentate gyrus, which includes the outer (*o*), middle (*m*), and inner (*i*) thirds of the stratum moleculare (*sm*), stratum granulosum (*sg*), and hilus (*hi*). Scale bar, 0.16 mm.

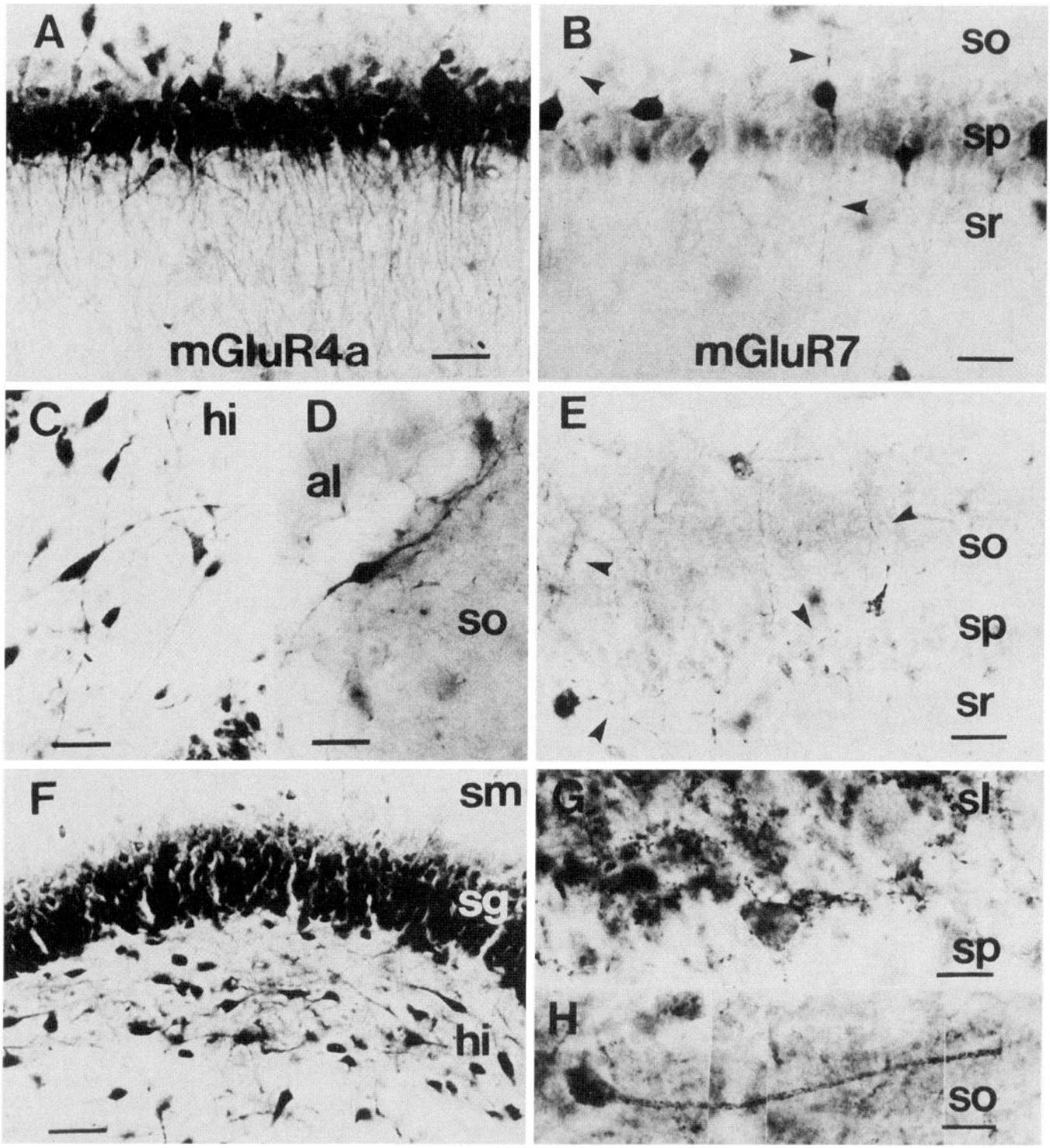

Figure 6. High-magnification light micrograph of mGluR4a and mGluR7 immunoreactivity in the hippocampal formation. *A* and *B* show immunoreactivity with mGluR4a and mGluR7 antibodies in the CA1 field: stratum oriens (*so*), stratum pyramidale (*sp*), and stratum radiatum (*sr*). *E* shows mGluR7 immunoreactivity in a similar section in area CA3. Note the punctate fibers stained with mGluR7-directed antibodies (*arrowheads*) in *B* and *E*. *C* and *D*, respectively, show high-magnification images of interneurons stained with mGluR4a-directed antibodies in the dentate hilus (*hi*) and a region of area CA1 containing the alveus (*al*) and the stratum oriens (*so*). A basket horizontal cell is shown that is immunopositive for mGluR4a in the hilus (*C*). In *D*, the presence of mGluR4a immunoreactivity is shown in a horizontal neuron at the border between alveus and stratum oriens. In *F*, cell bodies of granule cells are immunopositive for mGluR4a antibodies: stratum moleculare (*sm*), stratum granulosum (*sm*), and hilus (*hi*). In *G*, mossy fibers immunopositive to mGluR7 are terminating on CA3 pyramidal neurons: stratum lucidum (*sl*) and stratum pyramidale (*sp*). *H* shows punctate staining reminiscent of presynaptic terminals on a somata and dendrite of an interneuron in the stratum oriens (*so*) in the CA3 area. Scale bar: *B–D*, 0.028 mm; *A*, *E*, *F*, 0.04 mm; *G*, 0.0012 mm; *H*, 0.018 mm.

band in rat brain homogenates that have been treated with deglycosylating enzymes.

Immunocytochemical distribution of mGluR4a in the hippocampus

Affinity-purified antibodies were used for immunocytochemical localization of mGluR4a and mGluR7 in the hippocampus. Antibodies directed against both mGluR4a and mGluR7 selectively stained different neuronal elements in the hippocampal formation (Fig. 4*A,B*). Immunoreactivity was virtually abolished when the affinity-purified antibodies were preabsorbed with the homologous peptide (Fig. 4*C,D*), but was unchanged when the antibodies were preabsorbed with the peptide corresponding to the C-terminal amino acid sequence of the other mGluR subtype (Fig. 4*E,F*). Furthermore, there was no appreciable staining with preimmune serum (data not shown). Taken together with the high specificity of each of the antibodies demonstrated in the Western blot analysis, these data suggest that each antibody is reacting selectively with either mGluR4a or mGluR7.

Immunoreactivity with mGluR4a and mGluR7 antibodies revealed distinct and somewhat complementary distributions in the rat hippocampus (Fig. 4*A,B*). mGluR4a immunoreactivity is intense in the cell body layers of all major subsectors (CA1, CA3, and dentate gyrus) of the hippocampal formation (Fig. 4*A*). There is also less dense mGluR4a immunoreactivity in the molecular layers of both the hippocampus proper (cornu ammonis) and the dentate gyrus. Higher magnification reveals that immunoreactivity for this receptor is highly localized on the cell bodies and apical dendrites of pyramidal neurons throughout areas CA1–CA4 (Figs. 5, 6*A*) and cell bodies of granule cells in the dentate gyrus (Figs. 5, 6*F*). In addition, a number of scattered interneurons are immunopositive for mGluR4a (Figs. 5, 6*D*); these are present in all layers of the hippocampus proper and are most prominent in the stratum oriens/alveus. As shown in Figure 6*D*, interneurons in the stratum oriens/alveus region that were immunopositive for mGluR4a often had processes oriented in a direction that was parallel to the cell body layer. Their morphology resembles the interneurons described previously by McBain et al. (1994). Interneurons that were immunopositive for mGluR4a were especially prevalent in the hilus region of the dentate gyrus (Figs. 5, 6*C*). Figure 6*C* shows mGluR4a immunostaining of horizontal basket cells in the hilus at a high magnification.

Most pyramidal cells in CA1 and CA3 that were examined for mGluR4a immunoreactivity by EM contained abundant DAB reaction product (Fig. 7*A*), which was found free in the cytoplasm and associated with endoplasmic reticulum and Golgi apparatus. Nuclei were not stained, and there was no particular association of reaction product with perikaryal cell membranes. Immunoreactive somata received symmetrical and occasional asymmetrical synapses formed by axon terminals that were often immunoreactive as well (Figs. 7*B,C*). The apical (Fig. 7*D*) and basal dendrites of the pyramidal cell were labeled extensively with reaction product that diffusely filled them, surrounding organelles and cytoskeletal elements. Many smaller spiny dendrites and dendritic spines were evident in the neuropil, consistent with smaller pyramidal cell dendrites (Fig. 7*E–M*). In smaller-caliber dendrites, immunoreaction product was more patchy and occasionally seemed to be concentrated postsynaptically at probable excitatory (i.e., asymmetrical) synapses (Fig. 7*E*). Well labeled dendrites frequently gave rise to unlabeled spines (Fig. 7*F*). In contrast, many dendrites gave rise to very densely labeled dendritic spines (Fig. 7*G,H*), and individual dendrites giving rise to both labeled and unlabeled dendrites were identified occasionally (Fig. 7*I*). Immunoreactive dendritic spines and their postsynaptic densities were intensely labeled. Most of the synapses received by labeled spines were from unlabeled axon terminals forming asymmetrical synapses (Fig. 7*G,I–K*), although a small number of mGluR4-immunoreactive terminals making asymmetrical (Fig. 7*H*) and, rarely, symmetrical synapses (Fig. 7*M*) with labeled spines were also identified. Interestingly, although mGluR4-immunoreactive terminals synapsing with spines were common, most of the postsynaptic spines were unlabeled (Fig. 7*J–L*).

mGluR4-immunoreactive myelinated axons (Fig. 8*A*), preterminal axons, and axon terminals were quite frequent in the neuropil in CA1 and CA3. Reaction product was diffusely located, surrounding synaptic vesicles and mitochondria. In some axon terminals, reaction product was especially dense near the synaptic active zone. The majority of mGluR4-immunoreactive terminals formed asymmetrical synapses that were with pyramidal cell somata (Fig. 7*B*) and labeled and unlabeled dendritic shafts (Fig. 8*B,D,E*) and spines (Fig. 7*H,J–L*). Many of the axodendritic synapses were with mGluR4-immunoreactive dendrites (Fig. 8*D*); however, unlabeled aspiny dendrites were observed that received an extremely high density of immunoreactive synapses (Fig. 8*C*). A significant number of mGluR4a-immunoreactive terminals formed symmetrical synapses with unlabeled (Fig. 8*E,F*) and labeled (Fig. 8*G*) dendrites. In CA3, mossy fiber terminals were identified by their large size (Fig. 8*H–J*), and most were immunoreactive, as were many of the spines with which they synapsed.

Immunocytochemical distribution of mGluR7 in the hippocampus

The pattern of staining with antibodies directed against mGluR7 was markedly different from the pattern of mGluR4a immunoreactivity. mGluR7 immunoreactivity was very light or absent from the cell bodies and proximal dendrites of pyramidal cells of the hippocampus proper and the granule cells of the dentate gyrus (Figs. 4*B*, 5). The neuropil regions of Ammon's horn and dentate gyrus, however, were densely immunoreactive. In both dentate gyrus and hippocampus proper, mGluR7 immunoreactivity was detected in fine fibers and puncta (Figs. 6*B,E*) (areas CA1 and CA3, respectively). In area CA1, mGluR7 staining was most intense in the stratum radiatum and considerably less intense in the stratum lacunosum-moleculare, and a narrow band of slightly darker immunoreactivity can be seen at the border of these two layers (Fig. 4*B*). This is in stark contrast with area CA3 in which immunoreactivity in the stratum radiatum is similar to that in CA1, but there is unusually intense mGluR7 immunoreactivity in the stratum lacunosum-moleculare (Fig. 4*B*). In addition, CA3 shows intense punctate staining of the stratum lucidum (Fig. 6*G*). In the stratum radiatum and stratum oriens of area CA3, mGluR7 is also expressed in puncta scattered along the somata and dendrites of interneurons (Fig. 6*H*).

In dentate gyrus, mGluR7 immunoreactivity follows a pattern similar to that in Ammon's horn. There was little or no staining of cell bodies or proximal dendrites of the granule cells (Figs. 4*B*, 5), but there was intense staining of neuropil regions. In the molecular layer, there was a clear demarcation of immunoreactivity with intense staining in the middle third of the molecular layer and light staining in the inner third. In contrast, immunoreactivity in the outer third of the molecular layer was virtually absent. There was also moderate to intense staining for mGluR7 in the hilus. As with the hippocampus proper, mGluR7 immunoreactivity in the molecular layer and hilus of the dentate gyrus was often punctate

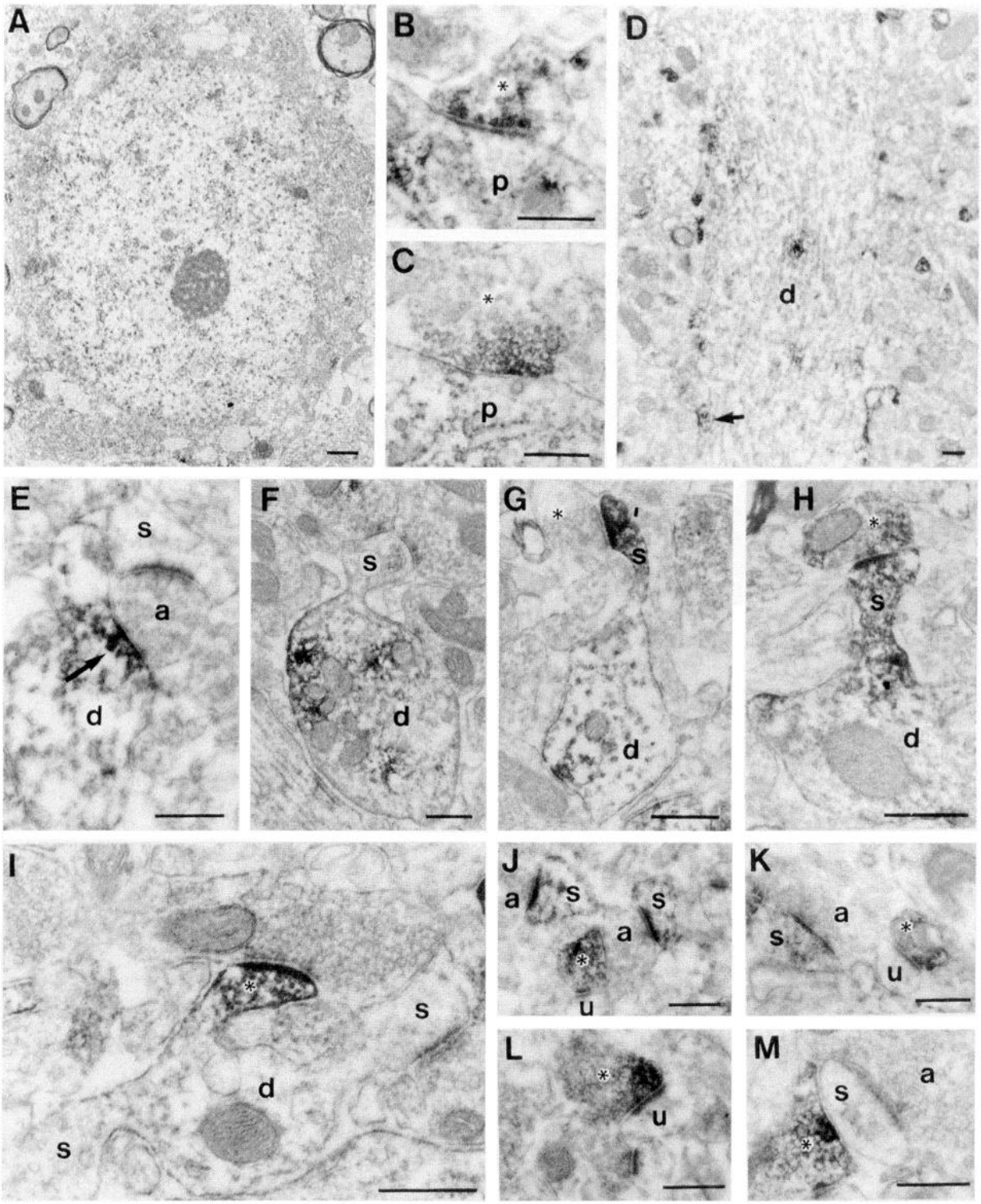

Figure 7. Electron micrographs demonstrating postsynaptic mGluR4a immunoreactivity in CA1 and CA3. *A* is an example of a densely labeled pyramidal cell in CA3. Reaction product is visible, filling the perikaryal cytoplasm. Immunoreactive axon terminals (*asterisks*) forming asymmetrical and symmetrical synapses with labeled pyramidal cells (*p*) in CA1 and CA3 are shown in *B* and *C*, respectively. An example of a labeled pyramidal cell apical dendrite (*d*) from CA1 is shown in *D*. Note the many axon terminals and dendritic spines visible in the surrounding neuropil. A dense patch of immunoreaction product near the plasma membrane at a synapse is evident (*short arrow*). Another such patch in a smaller CA1 dendrite (*d*) observed in *E* is postsynaptic to an axon terminal (*a*) synapsing with it (*arrow*) and with an unlabeled dendritic spine (*s*). *F* is an example of a well labeled dendrite (*d*) in CA3 giving rise to an unlabeled spine (*s*). *G* and *H* are examples of labeled CA3 dendrites (*d*) giving rise to intensely immunoreactive spines (*s*) postsynaptic to unlabeled and labeled axon terminals (*asterisks*), respectively. A minimally labeled CA3 dendrite (*d*) giving rise to one well labeled (*asterisk*) and two unlabeled spines (*s*) is shown in *I*. *J–L* are examples of axospinous synapses and contain three mGluR4a-immunoreactive spines (*s*) synapsing with unlabeled axon terminals (*a*) and three immunoreactive axon terminals (*asterisks*) synapsing with unlabeled spines (*u*). In *M*, an unlabeled dendritic spine (*s*) is postsynaptic to an unlabeled axon terminal (*a*) at an asymmetrical synapse and to a labeled axon terminal (*asterisk*) at a symmetrical synapse. Scale bar: *A*, 1000 nm; *B–M*, 400 nm.

and was prominent in fine fibers. In addition, there was prominent mGluR7 immunoreactivity in axons in the fimbria and fornix (Fig. 9). In contrast, there was no detectable staining of these fibers with antibodies directed against mGluR4a (Fig. 9).

As with mGluR4a immunoreactivity, staining for mGluR7 was also present in cell bodies of scattered interneurons in the hippocampus proper (Fig. 6*B*). In contrast to mGluR4a immunoreactivity, there was no detectable mGluR7 in interneurons in the dentate gyrus.

Immuno-EM analysis of mGluR7 immunoreactivity in stratum oriens, pyramidale, and lucidum in CA3 was consistent with the light-level analysis and revealed that labeling was predominately in axonal elements. Occasional pyramidal cells with light patches of perikaryal immunoreaction product (Fig. 10*A*) were observed, however, as were occasional well labeled dendrites and spines (Fig. 10*B,C*). Labeled axons were very common and included myelinated axons (Fig. 10*D*), preterminal axons, and axon terminals. Most intensely labeled were axon terminals, which formed asymmetrical synapses with pyramidal cell somata (Fig. 10*E*) and apical dendrites (Fig. 10*F*), spiny and aspiny dendrites (Fig. 10*G*), and dendritic spines (Fig. 10*H,I*). A population of aspiny dendrites was identified in stratum pyramidale and stratum radiatum, which were almost completely covered with mGluR7-immunoreactive terminals synapsing with them (Fig. 10*G*). Although the majority of mossy terminals was not labeled, a small percentage contained localized patches of reaction product (Fig. 10*J,K*), which was usually in the vicinity of synapses.

DISCUSSION

In recent years, a great deal of progress has been made in determining the physiological roles of mGluRs in the hippocampal formation. Little is known, however, about the specific physiological roles of each of the eight cloned mGluR subtypes. Development of a complete understanding of the regional, cellular, and subcellular distributions of each mGluR subtype will be essential for gaining insight into the specific roles of each receptor in regulating hippocampal function. Although information regarding the cellular distributions of mGluRs has been gleaned from *in situ* hybridization analysis (for review, see Testa et al., 1994), this method is limited in that it localizes mRNA rather than receptor proteins. After translation from mRNA in the cell body, receptor proteins are transported specifically to neuronal processes, where they function at sites far removed from their sites of synthesis. Furthermore, differences in protein turnover rates and/or translation efficiencies can result in large discrepancies between levels of a particular mRNA and its translation product. Receptor autoradiography cannot be used for localization of mGluR subtypes, because there are no selective ligands available for these receptors. Furthermore, receptor autoradiography does not have the resolution needed to localize receptors to individual perikarya, processes, and synapses. Another approach that has been used for localization of receptor subtypes with a great deal of success is immunocytochemistry using antibodies that react with specific receptor-protein subtypes (Levey et al., 1991; Blackstone et al., 1992; Martin et al., 1992; Ciliax et al., 1994; Hersch et al., 1995).

In the present studies, we have developed antibodies specific for two group III mGluR subtypes, mGluR4a and mGluR7. Several experiments suggest that each of these antibodies reacts in a highly specific manner with the targeted receptor. Western blot analysis revealed that both antibodies selectively recognize proteins in cell lines transfected with the appropriate receptor cDNAs but not in nontransfected cells or cell lines transfected with other mGluR subtypes. Each antibody also recognizes native proteins in rat brain homogenates with molecular weights consistent with the molecular weights of the immunoreactive proteins in transfected cell lines. Finally, preadsorption of the antibodies with the homologous peptides abolished all the immunoreactive bands, suggesting that the antibodies were reacting with the targeted epitope rather than binding nonspecifically.

Western blot analysis of the distribution of mGluR7 immunoreactivity in various dissected regions of rat brain revealed a distribution of this protein that is in close agreement with the previously reported distribution of mGluR7 mRNA (Okamoto et al., 1994; Saugstad et al., 1994), including intense mGluR7 immunoreactivity in cortical and olfactory regions, low immunoreactivity in pons/medulla, and absence of immunoreactivity in cerebellum. In contrast, there was no clear correlation between the distribution of mGluR4 mRNA (Tanabe et al., 1993) and mGluR4a immunoreactivity. mGluR4a immunoreactivity was somewhat uniform throughout the different brain regions examined, whereas mGluR4 mRNA is high in cerebellum and olfactory bulb and relatively low in other brain regions. The reason for this discrepancy is unclear. One possibility is that this reflects different distributions of the two splice variants of mGluR4 (mGluR4a and mGluR4b). For example, if mGluR4b is highly expressed in cerebellum and olfactory bulb, this could explain the high levels of mGluR4 mRNA in these structures. Another possible explanation for these data is that there may be an unusually high turnover rate or a low translation efficiency for mGluR4 in cerebellum and olfactory bulb that leads to a discrepancy between relative protein and mRNA levels. Also, discrepancies between mRNA and protein distributions can be attributed to transport of proteins to sites distal to the original site of synthesis. Finally, as with any immunocytochemical procedure, it is never possible to be certain that the reaction product is localized only to the molecule of interest. Thus, it is possible that the mGluR4a-directed antibodies also react with another protein in the tissue sections. The high specificity of the mGluR4a antibodies demonstrated in Western blot studies, however, coupled with the finding that the only immunoreactive product has a molecular weight that is consistent with mGluR4a and the ability to abolish immunoreactive staining of sections with peptides homologous to the receptor sequence, increases confidence that the immunocytochemical staining represents mGluR4a protein.

The immunocytochemical localization of mGluR4a and mGluR7 in the rat hippocampus may provide valuable insights into the possible physiological roles of these receptors. As discussed above, mGluRs 4, 6, 7, and 8 are all selectively activated by L-AP4 and comprise the group III mGluRs. One of the most prominent physiological effects of group III mGluR activation is reduction of transmission at glutamatergic synapses by reduction of glutamate release from presynaptic terminals (for review, see Glaum and Miller, 1994). In the hippocampus, L-AP4-sensitive presynaptic mGluRs are involved in reducing transmission at each of the three major excitatory synapses (Koerner and Cotman, 1981; Lanthorn et al., 1984; Baskys and Malenka, 1991; Gereau and Conn, 1995a). The present finding that both mGluR4a and mGluR7 are localized presynaptically at asymmetrical (presumably glutamatergic) synapses in the hippocampus suggests that both of these receptors could serve as presynaptic autoreceptors involved in regulating glutamate release.

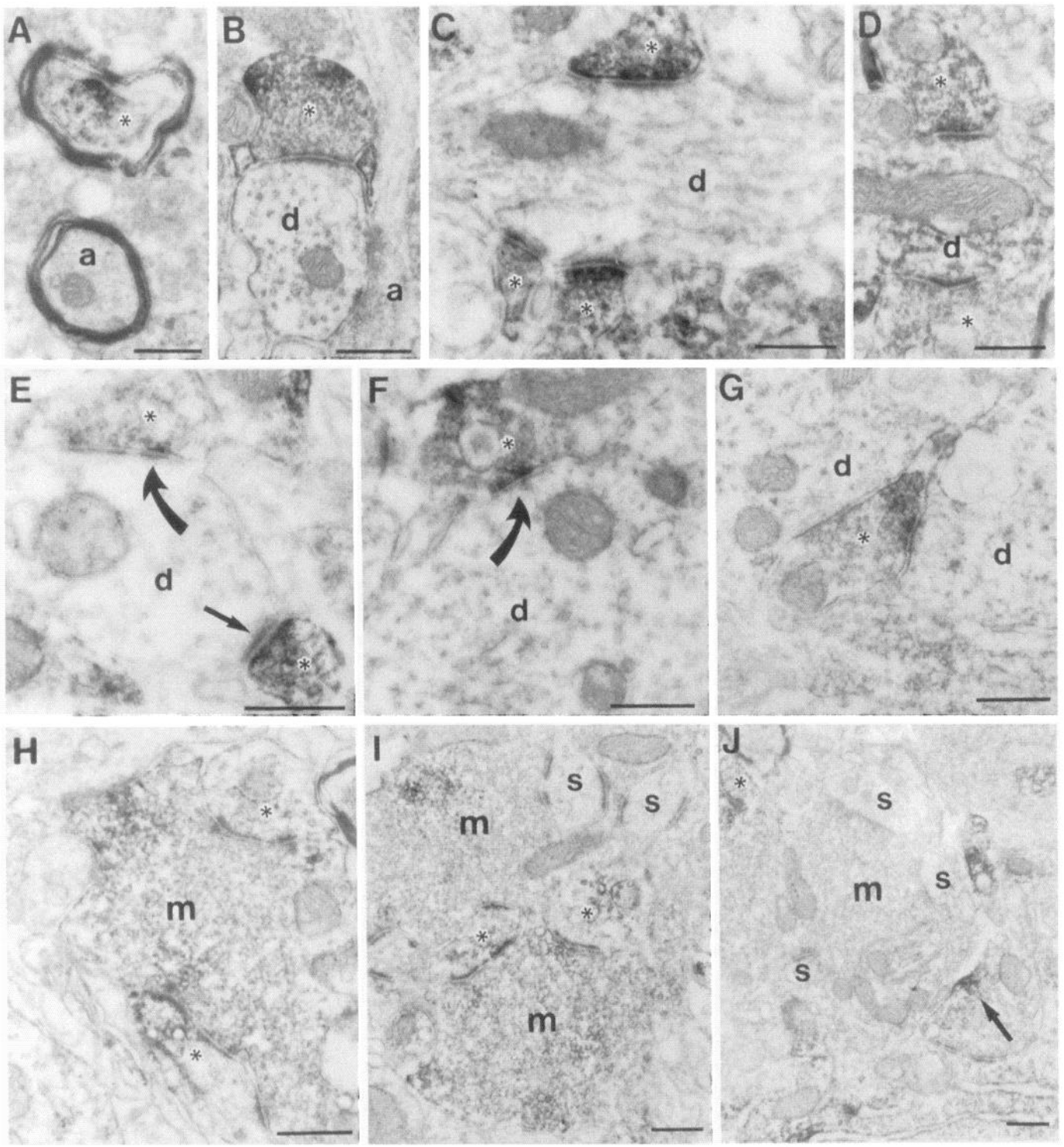

Figure 8. Electron micrographs demonstrating presynaptic mGluR4a immunoreactivity in CA1 and CA3. *A* demonstrates immunoreactive (*asterisk*) and unlabeled (*a*) myelinated axons in CA1. *B*, An unlabeled dendrite (*d*) in CA3 receiving synapses from labeled (*asterisk*) and unlabeled axon terminals (*a*). Most of the reaction product in the labeled terminal is away from the synaptic active zone. In *C*, an unlabeled CA3 dendrite (*d*) forms asymmetrical synapses with three mGluR4a-immunoreactive axon terminals (*asterisks*). Reaction product in these terminals is concentrated at the synaptic active zones. In *D*, an immunoreactive CA3 dendrite (*d*) is postsynaptic to two labeled axon terminals (*asterisks*). *E–G* are examples of dendrites (*d*) receiving symmetrical synapses from mGluR4-immunoreactive axon terminals (*asterisks*). In *E* and *F*, unlabeled CA1 dendrites (*d*) receive two symmetrical (*curved arrows*) and one asymmetrical (*straight arrow*) synapse. In *G*, two immunoreactive CA3 dendrites (*d*) are forming symmetrical synapses with one mGluR4 terminal (*asterisk*). *H–J* are examples of mossy fiber terminals (*m*) in CA3 forming multiple synapses with labeled (*asterisks*) and unlabeled spines (*s*). The mossy terminals in *H* and *I* are well labeled, whereas the one in *J* has only a single patch of reaction product (*arrow*). Scale bars, 400 nm.

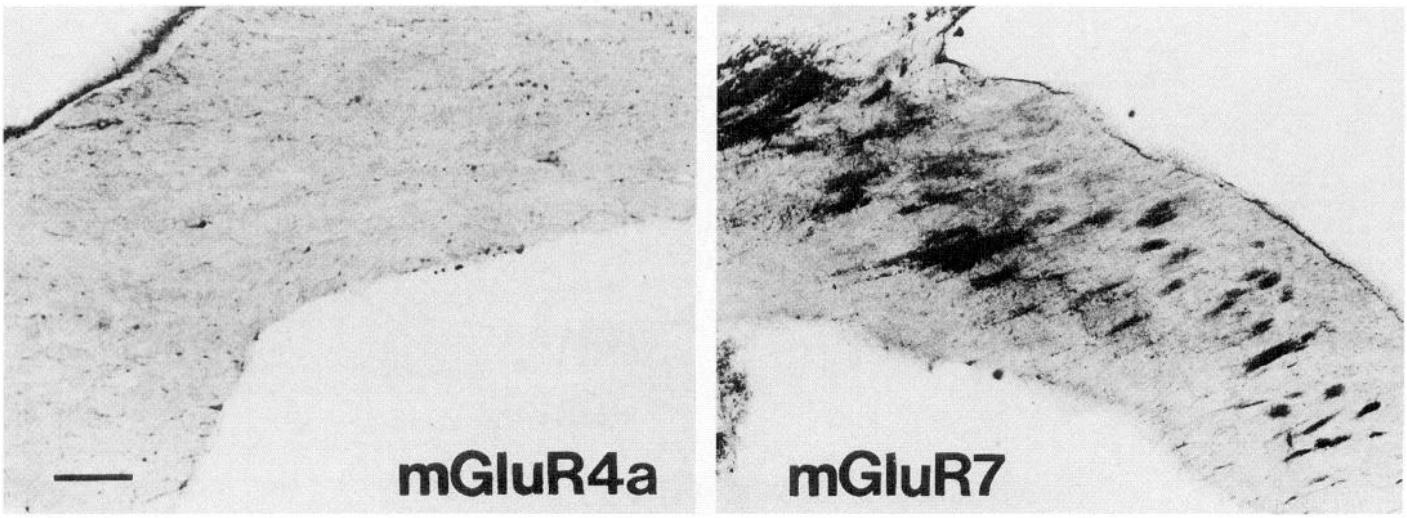

Figure 9. Immunoreactivity of mGluR4a and mGluR7 in the fimbria. Bundles of axons are immunopositive with antibodies directed against mGluR7 but not mGluR4a. Scale bar, 0.15 mm.

Although both mGluR4a and mGluR7 were presynaptically localized on excitatory synapses, there were some interesting differences between the localization of these two mGluR subtypes. For instance, both receptors are presynaptically localized at excitatory synapses in area CA3 but mGluR4a is heavily localized at mossy fiber synapses, whereas mGluR7 immunoreactivity was primarily localized on nonmossy fiber asymmetrical synapses. This suggests that mGluR4a may serve as an autoreceptor on mossy fiber terminals, whereas mGluR7 may be an autoreceptor at excitatory synapses from commissural, recurrent, and/or perforant path projections to CA3 pyramidal cells. Consistent with this hypothesis, L-AP4 reduces transmission at the mossy fiber synapse in rats (Lanthorn et al., 1984). The concentrations of L-AP4 required for reducing transmission at this synapse are higher than would be expected for mGluR4a, however, and a rigorous pharmacological characterization of the autoreceptors at this synapse has not been performed. Consistent with the possibility of mGluR7 localization on terminals from perforant path and commissural afferents, there was intense mGluR7 (but not mGluR4a) immunoreactivity in axons in the fimbria/fornix, which contains excitatory commissural afferents. Also, there was intense mGluR7 staining in the stratum lacunosum-moleculare of area CA3, where fibers from perforant path projections to the hippocampus terminate (Lorente de No, 1934; Raisman et al., 1965; Steward, 1976; Witter, 1986). Likewise, mGluR7 immunoreactivity was intense in the middle third of the molecular layer of the dentate gyrus, where afferents from the medial perforant path terminate with dentate granule cells (Teyler and DiScenna, 1984).

Another important difference between presynaptic staining with mGluR4a and mGluR7 antibodies was that mGluR7 immunoreactivity was localized exclusively at asymmetrical synapses, suggesting localization only on glutamatergic terminals, whereas mGluR4a immunoreactivity was localized presynaptically on both asymmetrical and symmetrical synapses. This suggests that mGluR4a also may play a role as a presynaptic heteroceptor involved in regulating transmission at inhibitory synapses. The source of the immunoreactive terminals at symmetrical synapses may be the immunoreactive interneurons that were seen at the light level.

In addition to its presynaptic localization, mGluR4a immunoreactivity was highly localized to cell bodies and apical dendrites of pyramidal cells, cell bodies of dentate granule cells, and cell bodies and dendrites of interneurons in both the hippocampus proper and dentate gyrus. Consistent with this, immuno-EM revealed heavy postsynaptic localization of mGluR4a at asymmetrical synapses onto pyramidal cells. Although mGluR7 immunoreactivity was primarily presynaptic, mGluR7 immunoreactivity was also seen occasionally on postsynaptic elements. It is possible that the well labeled spiny dendrites are related to the mGluR7-immunopositive interneurons seen at the light level, suggesting that mGluR7 may play a postsynaptic role in these neurons. Also, preliminary studies in nonhippocampal regions suggest that mGluR7 may have a substantial postsynaptic localization in some brain regions (unpublished findings). The finding of postsynaptic group III mGluRs is surprising in light of the prevailing view that the major role of group III mGluRs is as presynaptic autoreceptors, and it suggests that these receptors may also play postsynaptic roles. Interestingly, we have reported that none of the previously described excitatory effects of mGluR activation in hippocampal pyramidal cells are elicited by selective agonists of group III mGluRs (Gereau and Conn, 1995b). Previous studies, however, suggest that group III mGluRs are coupled to inhibition of adenylyl cyclase (for review, see Conn et al., 1995), and it is possible that these receptors are involved specifically in regulation of cAMP-mediated responses.

In summary, mGluR4a and mGluR7 subtype-specific antibodies have been developed and used for immunocytochemical localization of these receptors in the hippocampal formation. Our studies suggest highly complementary distributions of these two receptor subtypes with a predominantly presynaptic localization of mGluR7 at glutamatergic synapses, presynaptic localization of mGluR4a at both excitatory and inhibitory synapses, and postsynaptic localization of mGluR4a in pyramidal cells, granule cells, and scattered interneurons. Additional electrophysiology and pharmacology studies will be needed to characterize further the presynaptic and postsynaptic functions of these receptors at each of the synapses in which immunoreactivity was revealed.

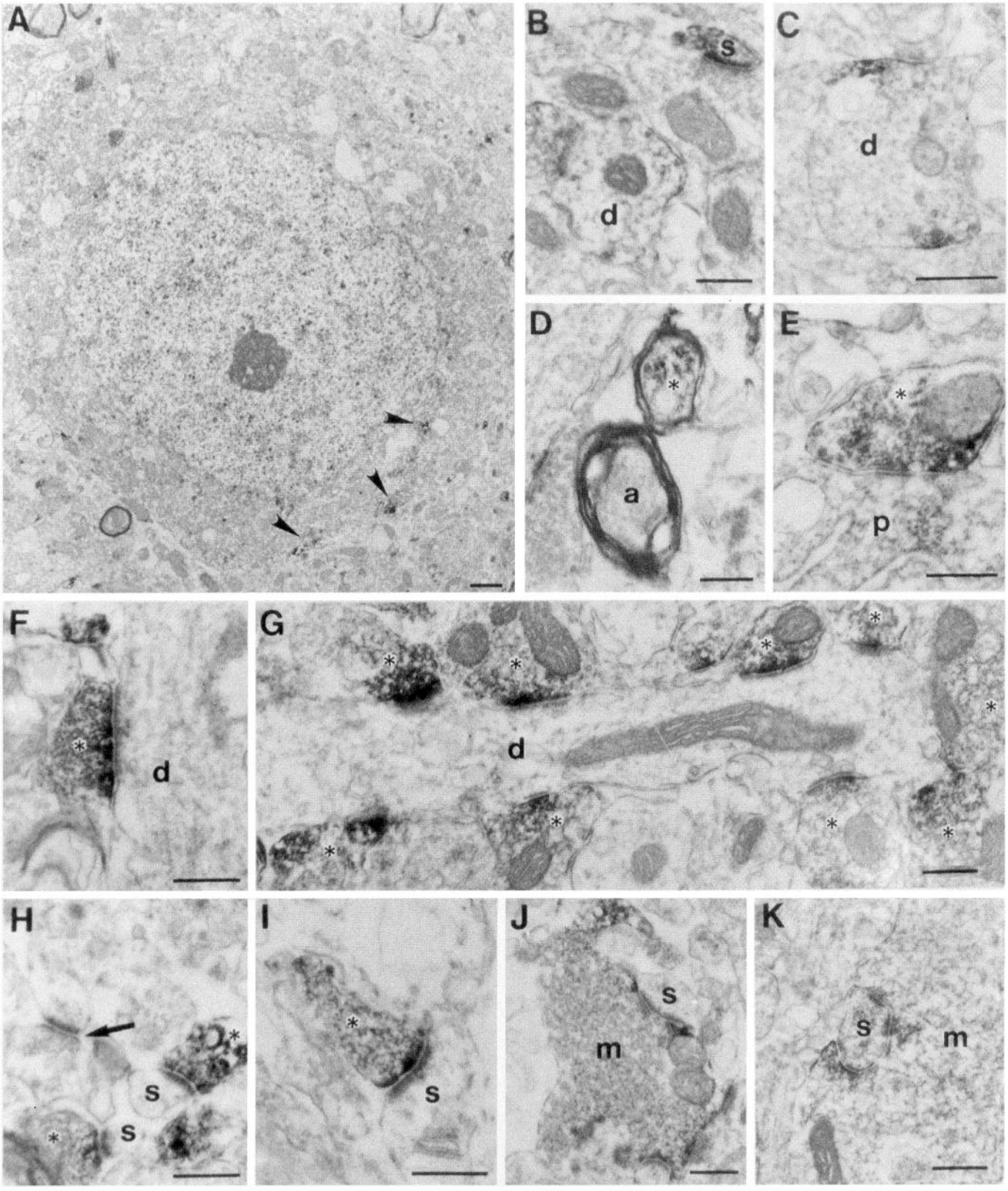

Figure 10. Electron micrographs demonstrating mGluR7 immunoreactivity in CA3. In *A*, a pyramidal cell somata is shown with a few patches of immunoreaction product (*arrowheads*). *B* and *C* are examples of uncommon immunoreactive dendrites (*d*) and a dendritic spine (*s*). *D* demonstrates immunoreactive (*asterisk*) and unlabeled (*a*) myelinated axons. *E* and *F* are examples of mGluR7-immunoreactive axon terminals (*asterisks*) synapsing with a pyramidal cell perikaryon (*p*) and an apical dendrite (*d*). *G* is the dendrite of a nonpyramidal cell (*d*) synapsing with at least eight mGluR7-immunoreactive axon terminals (*asterisks*). *H* and *I* are examples of mGluR7 axon terminals (*asterisks*) synapsing with dendritic spines (*s*). An unlabeled axospinous synapse (*arrow*) is visible in *H* for comparison. *J* and *K* are examples of minimally labeled mossy fiber axon terminals (*m*), synapsing with several spines (*s*). Scale bars: *A*, 1000 nm; *B–K*, 200 nm.

REFERENCES

Baskys A, Malenka RC (1991) Agonists at metabotropic glutamate receptors presynaptically inhibit EPSCs in neuronal rat hippocampus. J Physiol (Lond) 444:687–701.

Blackstone CD, Moss SJ, Martin LJ, Levey AI, Price DL, Hugarin RL (1992) Biochemical characterization and localization of a non-*N*-methyl-D-aspartate glutamate receptor in rat brain. J Neurochem 58:1118–1126.

Blumberg JB, Vetulani J, Stawarz RJ, Sulser F (1976) The noradrenergic cyclic AMP generating system in the limbic forebrain: pharmacological characterization in vitro and possible role of limbic noradrenergic mechanisms in the mode of action of antipsychotics. Eur J Pharmacol 37:357–366.

Brown TH, Zador AM (1990) Hippocampus. In: The synaptic organization of the brain (Shepherd GM, ed), pp 346–388. New York: Oxford UP.

Ciliax BJ, Hersch SM, Levey AI (1994) Immunocytochemical localization of D1 and D2 receptors in rat brain. In: Dopamine receptors and transporters: pharmacology, structure, and function (Niznik HB, ed), pp 383–399. New York: Marcel Dekker.

Conn PJ, Winder DG, Gereau IV RW (1994) Regulation of neuronal circuits and animal behavior by metabotropic glutamate receptors. In: The metabotropic glutamate receptors (Conn PJ, Patel J, eds), pp 195–229. Totowa, NJ: Humana.

Conn PJ, Chung DS, Winder DG, Gereau RW, Boss V (1995) Biochemical transduction systems operated by excitatory amino acids. In: CNS neurotransmitters and neuromodulators (Stone W, ed), pp 181–200. Boca Raton, FL: CRC.

Duvoisin R, Zhang C, Ramonell K (1995) A novel metabotropic glutamate receptor expressed in retina and olfactory bulb. J Neurosci 15:3075–3083.

Ganong AH, Cotman CW (1982) Acidic amino acid antagonists of lateral perforant path synaptic transmission: agonist-antagonist interactions in the dentate gyrus. Neurosci Lett 34:195–200.

Gereau RW, Conn PJ (1995a) Multiple presynaptic metabotropic glutamate receptors modulate excitatory and inhibitory synaptic transmission in hippocampal area CA1. J Neurosci 15:6879–6889.

Gereau RW, Conn PJ (1995b) Roles of specific metabotropic glutamate receptor subtypes in regulation of hippocampal CA1 pyramidal cell excitability. J Neurophysiol 74:122–129.

Glaum SR, Miller RJ (1994) Acute regulation of synaptic transmission by metabotropic glutamate receptors. In: The metabotropic glutamate receptors (Conn PJ, Patel J, eds), pp 147–172. Totowa, NJ: Humana.

Glowinski J, Iversen L (1966) Regional studies of catecholamines in the rat brain. III. Subcellular distribution of endogenous and exogenous catecholamines in various brain regions. Biochem Pharmacol 15:977–987.

Hersch SM, Ciliax BJ, Gutekunst C-A, Rees HD, Heilman CJ, Yung KKL, Bolam JP, Ince E, Yi H, Levey AI (1995) Electron microscopic analysis of D1 and D2 dopamine receptor proteins in the dorsal striatum and their synaptic relationships with motor corticostriatal afferents. J Neurosci 15:5222–5237.

Koerner JF, Cotman CW (1981) Micromolar L-2-amino-4-phosphonobutyric acid selectively inhibits perforant path synapses from lateral entorhinal cortex. Brain Res 216:192–198.

Kristensen P, Suzdak PD, Thomsen C (1993) Expression pattern and pharmacology of the rat type IV metabotropic glutamate receptor. Neurosci Lett 155:159–162.

Lanthorn TH, Ganong AH, Cotman CW (1984) 2-Amino-4-phosphonobutyrate blocks mossy fiber-CA3 responses in guinea pig but not rat hippocampus. Brain Res 290:174–178.

Levey AI, Kitt CA, Simonds WF, Price DL, Brann MR (1991) Identification and localization of muscarinic acetylcholine receptor proteins in brain with subtype-specific antibodies. J Neurosci 11:3218–3226.

Lorente de No (1934) Studies on the structure of the cerebral cortex. II. Continuation of the study of the ammonic system. J Psychologie Neurologie 46:113–177.

Martin LJ, Blackstone CD, Huganir RL, Price DL (1992) Cellular localization of a metabotropic glutamate receptor in rat brain. Neuron 9:259–270.

McBain CJ, DiChiara TJ, Kauer JA (1994) Activation of metabotropic glutamate receptors differentially affects two classes of hippocampal interneurons and potentiates excitatory synaptic transmission. J Neurosci 14:4433–4445.

Nakajima Y, Iwakabe H, Akazawa C, Nawa H, Shigemoto R, Mizuno N, Nakanishi S (1993) Molecular characterization of a novel retinal metabotropic glutamate receptor mGluR6 with a high agonist selectivity for L-2-amino-4-phosphonobutyrate. J Biol Chem 268:11868–11873.

Okamoto N, Hori S, Akazawa C, Hayashi Y, Shigemoto R, Mizuno N, Nakanishi S (1994) Molecular characterization of a new metabotropic glutamate receptor mGluR7 coupled to inhibitory cyclic AMP signal transduction. J Biol Chem 269:1231–1236.

Pin J-P, Duvoisin R (1995) The metabotropic glutamate receptors: structure and function. Neuropharmacology 34:1–26.

Raisman G, Cowan WM, Powell TP (1965) The extrinsic afferent, commissural and association fibers of the hippocampus. Brain 88:963–998.

Saugstad JA, Kinzie JM, Mulvihill ER, Segerson TP, Westbrook GL (1994) Cloning and expression of a new member of the L-2-amino-4-phosphonobutyric acid-sensitive class of metabotropic glutamate receptors. Mol Pharmacol 45:367–372.

Steward O (1976) Topographic organization of the projections from the entorhinal area to the hippocampal formation of the rat. J Comp Neurol 167:285–314.

Suzdak PD, Thomsen C, Mulvihill E, Kristensen P (1994) Molecular cloning, expression, and characterization of metabotropic glutamate receptor subtypes. In: The metabotropic glutamate receptors (Conn PJ, Patel J, eds), pp 1–30. Totowa, NJ: Humana.

Tanabe Y, Nomura A, Masu M, Shigemotor R, Mizuno N, Nakanishi S (1993) Signal transduction, pharmacological properties, and expression patterns of two rat metabotropic glutamate receptors, mGluR3 and mGluR4. J Neurosci 13:1372–1378.

Testa CM, Catania MV, Young AB (1994) Anatomical distribution of metabotropic glutamate receptors in mammalian brain. In: The metabotropic glutamate receptors (Conn PJ, Patel J, eds), pp 99–123. Totowa, NJ: Humana.

Teyler TJ, DiScenna P (1984) The topological anatomy of the hippocampus: a clue to its function. Brain Res Bull 12:711–719.

Thomsen C, Mulvihill ER, Haldeman B, Pickering DS, Hampson DR, Suzdak PD (1993) A pharmacological characterization of the mGluR1a subtype of the metabotropic glutamate receptor expressed in a cloned baby hamster kidney cell line. Brain Res 619:22–28.

Towbin H, Staehelin T, Gordon J (1979) Electrophoretic transfer of proteins from polyacrylamide gels to nitrocellulose sheets: procedures and some applications. Proc Natl Acad Sci USA 76:4350–4354.

Witter MP (1986) A survey of the anatomy of the hippocampal formation, with emphasis on the septotemporal organization of its intrinsic and extrinsic connections. Adv Exp Med Biol 23:67–82.